THE JOURNAL OF BIOLOGICAL CHEMISTRY
Vol. 277, No. 37, Issue of September 13, pp. 33598–33603, 2002
Printed in U.S.A.

Trafficking of L-type Calcium Channels Mediated by the Postsynaptic Scaffolding Protein AKAP79*

Received for publication, March 14, 2002, and in revised form, June 12, 2002
Published, JBC Papers in Press, July 11, 2002, DOI 10.1074/jbc.M202476200

Christophe Altier,[a,b] Stefan J. Dubel,[a] Christian Barrère,[a] Scott E. Jarvis,[c,d] Stéphanie C. Stotz,[c,e] Renée L. Spaetgens,[c,f] John D. Scott,[g] Véronique Cornet,[h] Michel De Waard,[i] Gerald W. Zamponi,[c,j] Joël Nargeot,[a] and Emmanuel Bourinet[a,k]

From the [a]Physiopathologie des Canaux Ioniques, Institut de Génétique Humaine CNRS UPR1142, 141 Rue de la Cardonille, 34396 Montpellier Cedex 5, France, the [c]Department of Physiology and Biophysics, Neuroscience Research Group, University of Calgary, Calgary, Alberta T2N 4N1, Canada, the [g]Howard Hughes Medical Institute, Vollum Institute, Oregon Health & Science University, Portland, Oregon 97201, [h]INSERM U464, Faculté de Médecine Nord, Boulevard Pierre Dramard, 13916 Marseille, France, and [i]INSERM EMI99-31, 17 Rue des Martyrs, 38054 Grenoble Cedex 9, France

Accurate calcium signaling requires spatial and temporal coordination of voltage-gated calcium channels (VGCCs) and a variety of signal transduction proteins. Accordingly, regulation of L-type VGCCs involves the assembly of complexes that include the channel subunits, protein kinase A (PKA), protein kinase A anchoring proteins (AKAPs), and β2-adrenergic receptors, although the molecular details underlying these interactions remain enigmatic. We show here, by combining extracellular epitope splicing into the channel pore-forming subunit and immunoassays with whole cell and single channel electrophysiological recordings, that AKAP79 directly regulates cell surface expression of L-type calcium channels independently of PKA. This regulation involves a short polyproline sequence contained specifically within the II-III cytoplasmic loop of the channel. Thus we propose a novel mechanism whereby AKAP79 and L-type VGCCs function as components of a biosynthetic mechanism that favors membrane incorporation of organized molecular complexes in a manner that is independent of PKA phosphorylation events.

Voltage-gated calcium channels (VGCCs) are transmembrane proteins involved in the regulation of cellular excitability and Ca^{2+} homeostasis in excitable and non-excitable cells (1). They play a key role in numerous cellular functions including enzyme activation, muscle contraction, neurotransmitter release, and gene transcription. Molecular cloning has led to the isolation and functional expression of a number of subunits that form Ca^{2+} channels. Based on primary structure homology, these subunits are separated into three different families (2). High voltage-activated channels are comprised of the L-types (Ca_V1) and the N-, P/Q-, and R-types (Ca_V2). The third family (Ca_V3) is comprised of the members of the low voltage-activated/T-type Ca^{2+} channels. Although primarily gated by fluctuations of membrane potential, an essential aspect of the function of these channels is their capacity to respond to extracellular signals via membrane receptors and intracellular second messengers that, in turn, alter channel activity. As for many ionic channels, growing evidence indicates that the specificity and speed of these regulations require a promiscuous organization of the constitutive channel subunits with membrane receptors and complexes of intracellular molecules. In that context, the role of scaffolding proteins in orchestrating these networks is crucial.

Accordingly, the regulation of voltage-gated calcium channels by anchored pools of protein kinases is a key factor in controlling intracellular calcium levels. Efficient phosphorylation is accomplished through formation of kinase-channel complexes. For example, protein kinase A (PKA)[1] is anchored near L-type calcium channels by different AKAPs in brain, skeletal muscle, smooth muscle, and myocardium (3–5). Consequently these interactions are needed for the activity-dependent regulation of contractile force in skeletal muscle (6) or the β-adrenergic modulation of positive heart inotropism (5, 7). Furthermore, in heterologous systems, PKA-dependent phosphorylation of both α_{1C} ($Ca_V1.2$) and α_{1S} ($Ca_V1.1$) L-type channels does not appear to occur in the absence of AKAP proteins (5, 8, 9), although the extent of regulation observed in these studies with recombinant systems is much smaller compared with the magnitude recorded in native cells (1, 10).

Two distinct membrane-anchored AKAPs (AKAP15/18 and AKAP79/150) have been studied in that context, and a direct interaction between the skeletal muscle L-type channel α_{1S} and AKAP15 has been recently identified (11). Whereas AKAP15/18 is prominent in muscles, AKAP79/150 is abundantly expressed in neurons and has a pattern of localization similar to that of α_{1C} (12–15). A high proportion of AKAP79/150 and α_{1C} is concentrated in the primary branches of dendrites where they associate with β2-adrenergic receptors (16) to form postsynaptic signaling complexes that regulate synaptic transmission.

* This work was supported by a Fondation UPSA grant (to E. B.), by Association Francaise de lutte contre les Myopathies (AFM) and Association de la Recherche contre le Cancer grants (to J. N.), and by operating grants from the Heart and Stroke Foundation of Alberta and the Northwest Territories and Canadian Institutes of Health Research (CIHR) (to G. W. Z.). The costs of publication of this article were defrayed in part by the payment of page charges. This article must therefore be hereby marked "*advertisement*" in accordance with 18 U.S.C. Section 1734 solely to indicate this fact.
[b] Supported by a studentship award from the AFM.
[d] Holds an Alberta Heritage Foundation for Medical Research (AHFMR) M.D./Ph.D. studentship.
[e] Supported by studentship awards from the AHFMR and the CIHR.
[f] Supported by the AHFMR.
[j] Holds salary awards from the AHFMR and the CIHR.
[k] To whom correspondence should be addressed: Physiopathologie des Canaux Ioniques Institut de Génétique Humaine, CNRS UPR1142, 141 Rue de la Cardonille, 34396 Montpellier Cedex 5, France. Tel.: 33-499-61-99-36; Fax: 33-499-61-99-01; E-mail: emmanuel.bourinet@igh.cnrs.fr.

[1] The abbreviations used are: PKA, protein kinase A; AKAP, A-kinase anchoring protein; PP, polyprolines; Po, open probability; WT, wild-type; HA, hemagglutinin; TEA, tetraethylammonium; AMPA, α-amino-3-hydroxy-5-methylisoxazole-4-propionic acid.

In the present study, we have examined in heterologous expression models the effect of AKAP79 coexpression on α_{1C} calcium channel activity to further delineate the determinant of their interactions. We found that AKAP79 directly regulates the surface expression of α_{1C} but, surprisingly, independently of PKA activation. A proline-rich region contained within the α_{1C} II-III intracellular linker coordinates this effect. We propose that this sequence, common to various L-type channels, may act as an inhibitory motif that can be masked by AKAP79, favoring the delivery to the plasma membrane of preassembled L-type Ca^{2+} channel signaling complexes.

EXPERIMENTAL PROCEDURES

Molecular Biology—We have previously described the generation of chimeras between α_{1C} and α_{1E} (17). The II-III loops of α_{1C} and α_{1E} were amplified by PCR and subcloned into c-Myc/pcDNA3. A similar procedure was used to fuse AKAP79 or AKAP79Δ388 with a c-Myc epitope. Deletion of the PP motif on the α_{1C} II-III loop (amino acids 854 to 864) was created by overlapping PCR, using as template a wild-type α_{1C} cDNA engineered to contain two unique silent restriction sites (*MluI* and *Spe*I) flanking the II-III loop region (18). The amplified 780-base pair *MluI-Spe*I fragment was reintroduced into the template DNA. Accuracy of the different sequences was analyzed by sequencing (Genome Express) and restriction digests.

Transient Expression of Recombinant Calcium Channels—The following cDNA sequences inserted in expression vectors have been used (GenBank™ accession numbers), α_{1A}, M64373; α_{1C}, M67515; α_{1E}, L15453; β_{1b}, NM017346; β_{2a}, M80545; α_2-δ_{1b}, AF286488; α_{1G}, AF126965; α_{1H}, NM021098; AKAP79, NM004857. For transient expression in *Xenopus* oocytes, nuclear injection was performed as previously reported (19). When AKAP79 was coexpressed with the Ca^{2+} channel subunits, we used a ratio of 1 (AKAP), 3 (Ca^{2+} channel mix). When needed, this mix was supplemented with the II-III loop constructs at a ratio of 3 (cDNA mix), 1 (II-III loop). As control, the empty vector was used to obtain the same dilution. Oocytes were then incubated at 18 °C for 2–4 days in ND96 medium on rotating platform. For mammalian cell expression, human embryonic kidney (HEK) cells were used and transfected with calcium phosphate as described previously (17).

Electrophysiology—Macroscopic oocyte currents were recorded using a two-electrode voltage clamp as previously described (19) with 5 mM barium as charge carrier. An AxoPatch-200B amplifier (Axon Instruments) was used for cell-attached recordings with 7–12 MΩ sylgard-coated pipettes filled with a solution containing (in mM): 100 $BaCl_2$, 10 HEPES, pH 7.3. 1 μM FPL64176 was also added to the pipette solution to facilitate the resolution of single channel events. Oocytes were placed in a high potassium solution to reduce the membrane potential to 0 mV. Whole cell recordings in HEK cells were performed with an AxoPatch-200B amplifier using an external solution containing (in mM): 10 $BaCl_2$, 160 TEACl, 10 HEPES (pH to 7.4 with TEAOH). Pipettes of 1–2 MΩ resistance were filled with an internal solution containing (in mM): 110 CsCl, 3 $MgCl_2$, 10 EGTA, 10 HEPES, 3 Mg-ATP, 0.6 GTP (pH to 7.2 with CsOH). All chemicals used were purchased from Sigma except for the peptide Ht-31 provided by Dr. N. Lamb (Montpellier, France). Ht-31 was injected during the recording by an additional microelectrode. pCLAMP7 software was used for data acquisition; analysis was performed with pCLAMP6, Excel, and GraphPad Prism software. Results are presented as the mean ± S.E. and compared using Student's *t* test.

Surface Expression—Surface expression of α_{1C} protein was measured using the immunoassay recently described (20). The hemagglutinin (HA) epitope was inserted into the extracellular S5-H5 loop of domain II. Complementary oligonucleotides encoding the HA epitope flanked with extra amino acids to enlarge the loop were annealed to form an *MluI* adaptor and ligated into a unique silent *MluI* site introduced at base pair 2055 by site-directed mutagenesis on the α_{1C} cDNA. The amino acid sequence of the HA-tagged α_{1C} reads ^{680}DEMQ*TRH***YPYD-VPDYA***VTFDEMQ*TRRS^{706} at the epitope insertion site (HA epitope shown in bold type, extra residues are in italics). The epitope is therefore 12 amino acids distant from the S5 end and from the start of the H5. Two days after cDNA injection, currents were recorded. Oocytes were then placed for 30 min in ND96 with 1% bovine serum albumin to block unspecific binding, incubated for 60 min at 4 °C with 1 μg/ml rat monoclonal anti-HA antibody (3F10, Roche Molecular Biochemicals) in ND96–1% bovine serum albumin, washed at 4 °C, and incubated for 30 min at 4 °C with horseradish peroxidase-coupled secondary antibody (goat anti-rat FAB fragments, Jackson ImmunoResearch). After several washes with 1% bovine serum albumin for 60 min at 4 °C, individual oocytes were washed with normal ND96 solution at room temperature and then placed in 50 μl of SuperSignal® ELISA Femto substrate (Pierce). Chemiluminescence was quantified immediately in a Luminoskan microplate reader (Labsystems Inc., Finland). All data were normalized to the level of signal obtained for the HA-α_{1C} channel complex with its ancillary α_2-δ and β_{1b} subunits.

Western Blotting—Oocytes protein samples were prepared as follows. Oocytes were homogenized in a buffer containing 100 mM NaCl, 20 mM Tris-HCl (pH 7.4), 1% Triton X-100, 1 mM phenyl-methylsulfonyl fluoride, supplemented with a protein inhibitor mix (Roche Diagnostics). Homogenates were shaken for 15 min at 4 °C and centrifuged at 14000 × *g* for 2 min. HEK samples were prepared as in Ref. 21. Proteins were separated by SDS-PAGE on 6 or 8% gels, transferred onto nitrocellulose membranes, and then immunoblotted. The blot was blocked with 5% powdered nonfat milk. c-Myc-tagged proteins were detected with mouse monoclonal anti-c-Myc antibodies at 1:300 dilution (9E10, Santa Cruz Biotechnology). HA-tagged proteins were detected with a rat monoclonal anti-HA antibody at 1:1000 dilution (3F10, Roche Molecular Biochemicals). Horseradish peroxidase-conjugated secondary antibodies at 1:5000 dilution (sheep anti-mouse, Amersham Biosciences, or goat anti-rat FAB fragments, Jackson ImmunoResearch) and the ECL chemiluminescence system (Amersham Biosciences) were used for detection.

RESULTS

AKAP79 Up-regulates L-type Current Density—When coexpressed with AKAP79, α_{1C} channels exhibited a 2 to 4-fold increase in current density (Fig. 1*A*). This augmentation was not associated with any significant changes in whole cell current kinetics nor with a leftward shift in the voltage dependence of activation, unlike what is typically seen following PKA-dependent regulation of native L-type calcium currents (Fig. 1*B*, α_{1C} α_2-δ β_{1b}, $V_{0.5}$ = −12.5 ± 0.5 mV, n = 20; α_{1C} α_2-δ β_{1b} + AKAP79, $V_{0.5}$ = −13.8 ± 0.4 mV, n = 19). The AKAP79-mediated enhancement of current amplitude did not require the presence of a calcium channel β_{1b} subunit (Fig. 1, *B* and *C*; +β_{1b}, I_{AKAP}/I = 3.1 ± 0.2, n = 26; −β_{1b}, I_{AKAP}/I = 2.9 ± 0.5, n = 8) and was not altered following coexpression of distinct forms of β-subunits (not shown), indicating that the effect of AKAP79 is intrinsic to the L-type calcium channel α_1 subunit. Moreover, coexpression of AKAP79 had no effect on the current amplitudes of members of the Ca_V2 (α_{1A}, α_{1E}) or Ca_V3 (α_{1G}, α_{1H}) calcium channel subfamilies (Fig. 1*C*), indicating that AKAP79 selectively affects L-type calcium channels.

One well characterized function of AKAPs is to bring PKA to the vicinity of its substrates to allow their phosphorylation, as observed for a number of ionic channels and plasma membrane-anchored AKAPs (22). To test whether activation of PKA that was associated with AKAP79 mediated enhancement of L-type channel currents, we applied several pharmacological agents that perturb PKA-dependent phosphorylation. First of all, long term incubation (24 h) of the oocytes with the broad spectrum protein kinase inhibitor H7 (100 μM) did not significantly alter the magnitude of the AKAP effect (Fig. 1*D*), suggesting that tonic channel phosphorylation is unlikely to underlie the up-regulation of L-type currents. Second, the stimulation of the PKA cascade by an acute application of 50 μM forskolin did not result in any functional change in α_{1C} channel activity in the presence (Fig. 1*D*) or absence of AKAP79. Third, to test whether the PKA-AKAP interaction is a prerequisite for the AKAP79 effects, we injected the oocytes during the time course of the recordings with the AKAPlbc-derived peptide Ht-31 (50 μM final concentration) that contains the critical RII-binding domain and is known to prevent association of PKA with AKAPs (23). As with H7 or forskolin, application of the Ht-31 peptide did not antagonize the AKAP79-induced current increase (Fig. 1*D*). Finally, we created a truncated AKAP79 construct in which the PKA-interacting RII domain had been deleted through insertion of a premature stop codon after residue 388 (Fig. 1*E*). In addition,

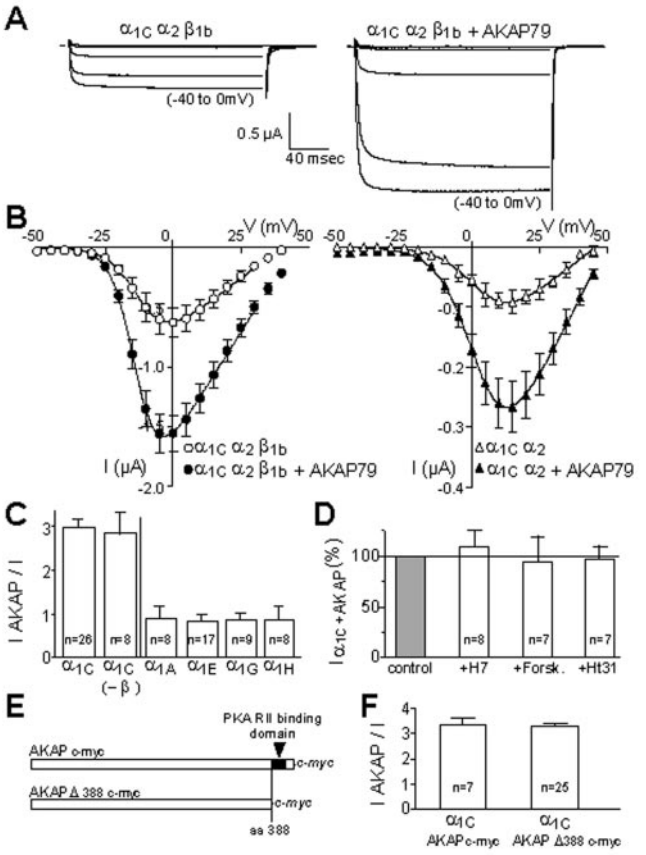

FIG. 1. **Coexpression of AKAP79 with α_{1C} L-type channels induces an increase in current amplitude.** *A*, typical current traces in response to 200-millisecond long depolarizations from −80 mV to five successive steps to −40, −30, −20, −10, and 0 mV. Note that AKAP79 does not alter current waveforms. *B*, current-voltage (I/V) relationships for α_{1C} + α_2-δ + β_{1b} ± AKAP79 and α_{1C} + α_2-δ ± AKAP79 (n = 8–24). *C*, mean AKAP effect on currents encoded by $\alpha_{1C,}$ $\alpha_{1A,}$ and α_{1E} (coexpressed with α_2-δ and β_{1b}), by α_{1C} + α_2-δ and by α_{1G} and α_{1H} (n = 8–26). Current amplitude was taken at the peak of the I/V curve in each case and plotted as ratios between AKAP-injected and non-injected batches. *D*, normalized current amplitude obtained following coexpression of α_{1C} + α_2-δ + β_{1b} and AKAP79 in control condition, after a 24-h incubation with 100 μM H7, after 10 min of treatment with forskolin (50 μM), or after injection of Ht-31 peptide (50 μM final concentration) (n = 7–8). *E*, topological representation of AKAP79 c-Myc and truncated AKAP79 Δ388 c-Myc. The *black boxes* represent the RII binding region. *F*, effects of AKAP79 c-Myc and AKAP79 Δ388 c-Myc on current amplitude of α_{1C} + α_2-δ + β_{1b} channels (n = 7 and 25). All *error bars* shown denote S.E.

both the mutant and the wild-type AKAP79 were fused to a c-Myc epitope to verify their expression. Consistent with the Ht-31 injections, both Δ388 and full-length AKAP79 promoted similar increases in α_{1C} channel activity (Fig. 1*F*, $I_{AKAP79\ c\text{-}Myc}/I$ = 3.36 ± 0.3, n = 7; $I_{AKAP79\Delta388\ c\text{-}Myc}/I$ = 3.28 ± 0.1, n = 26). Collectively, these data indicate that the ability of AKAP79 to enhance L-type calcium channel levels occurs independently of its role in PKA signaling, hinting at a novel action that might perhaps be related to its function as a scaffolding protein (24).

Unitary Conductance Is Not Affected—The increase in current level could in principle be due to one or a combination of three factors, single channel conductance, maximum open probability (Po), or an increase in the number of functional channels. To distinguish among these possibilities, we first examined the effect of the calcium channel agonist FPL64176, which is known to enhance the Po. If the major function of AKAP79 were due to a selective effect on Po, then one might expect a smaller FPL-mediated effect on channels coexpressed with AKAP79. The magnitude of FPL increase, however, was similar with or without AKAP (−AKAP, 3.08-fold ± 0.3, n = 7, +AKAP, 2.93-fold ± 0.3, n = 8). Although such observations would not be discriminative for small Po changes, they suggest that AKAP79 does not act in majority by increasing Po. Next, we performed cell-attached single channel recordings to examine a putative AKAP79 effect on unitary conductance (Fig. 2, *A* and *B*). In the presence of AKAP79, the number of channels per patch was consistently increased and the number of patches without channels reduced. However, the conductance remained unaltered (Fig. 2*B*). Thus, rather than changing channel function, AKAP79 appears to act by increasing channel density.

AKAP79 Promotes α_{1C} Plasma Membrane Expression—To determine whether AKAP79 indeed altered the plasma membrane expression of the channel complex, we directly measured plasma membrane protein levels based on the immunoassay described by Zerangue *et al.* (20). We inserted the HA epitope into the domain II S5-H5 extracellular loop of α_{1C}, and to ensure a good accessibility of the epitope we introduced extra flanking residues known to optimize the recognition by the antibody (25). The tagged channel was recognized by the anti-HA antibody in Western blots (Fig. 3*A*), and its currents were still augmented following AKAP79 coexpression. Moreover, its biophysical properties were identical to that seen with the wild-type (WT) channels, suggesting that the insertion of the additional sequence did not disrupt channel conformation. The assay to measure surface expression consists of an enzymatic amplification of HA recognition by using a peroxidase-coupled secondary antibody and a maximum sensitivity-enhanced chemiluminescent substrate adapted to luminometric detection. After electrophysiological recordings, individual non-permeabilized oocytes were processed with the primary and secondary antibodies. Channel surface expression on individual oocytes, directly related to the intensity of chemiluminescence, was subsequently quantified with a luminometer. For positive and negative controls we used an HA-tagged Kir2.1 potassium channel (known to give a good signal in this assay, Ref. 20) and the WT α_{1C} channel, respectively. As shown in Fig. 3*B*, the WT L-type channel alone yielded a signal no higher than background, whereas HA-Kir2.1 produced consistent chemiluminescence. Because the ancillary β-subunit is known to increase calcium current levels by disrupting an endoplasmic reticulum retention mechanism (26), we first tested the accuracy of the assay by asking whether coexpression of the β-subunit alters surface expression of the HA-α_{1C} subunit. Indeed, surface expression of HA-α_{1C} was increased by about 3-fold upon coexpression with β_{1b} (Fig. 3*B*). However, this could not account for all of the observed increase in current amplitude (~7-fold, Fig. 1*B*), consistent with the dual role of this regulatory subunit in controlling both the expression and the biophysical properties of the pore subunit (27). In contrast, coexpression of AKAP79 promotes a further increase in surface expression of the HA-α_{1C} (+α_2+β_{1b}) channel complex (2 ± 0.27-fold, Fig. 2*D*) that is consistent with the observed stimulation of current density. Thus, combination of electrophysiology and surface protein measurements supports the notion that AKAP79 appears to increase expression of α_{1C} in the plasma membrane.

Molecular Determinants of AKAP79-sensitive Trafficking—We tested a series of chimeric calcium channels (17, 19) to map the structural determinants in α_{1C} that increase current levels in the presence of AKAP79. We utilized a family of chimeric channels that were previously generated by switching transmembrane domains from the α_{1C} L-type channel with corresponding regions from the AKAP79-insensitive α_{1E} channel. Note that each domain that was swapped also contained the preceding intracellular loop (*i.e.* II-III loop with domain III). As shown in Fig. 4*A*, the effects of AKAP79 were main-

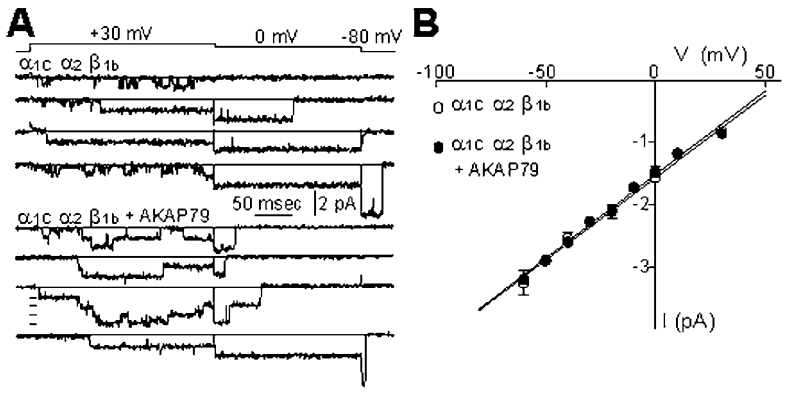

FIG. 2. **AKAP79 does not affect α_{1C} unitary conductance.** *A*, unitary channel records obtained from cell-attached patches from oocytes expressing α_{1C} + α_2-δ + β_{1b} ± AKAP79. 1 μM FPL64176 was included in the patch pipette to facilitate resolution of single channel events. Currents were elicited from a holding potential of −80 mV to test potentials of +30 and 0 mV. Long openings, typical of L-type channels in the presence of FPL64176, can be observed. Note that the number of channels is increased in the presence of AKAP79. *B*, lack of effect of AKAP79 on single channel conductance of α_{1C} + α_2-δ + β_{1b} (−AKAP, γ = 26.6 picosiemens, n = 3; + AKAP, γ = 26.9 picosiemens, n = 4).

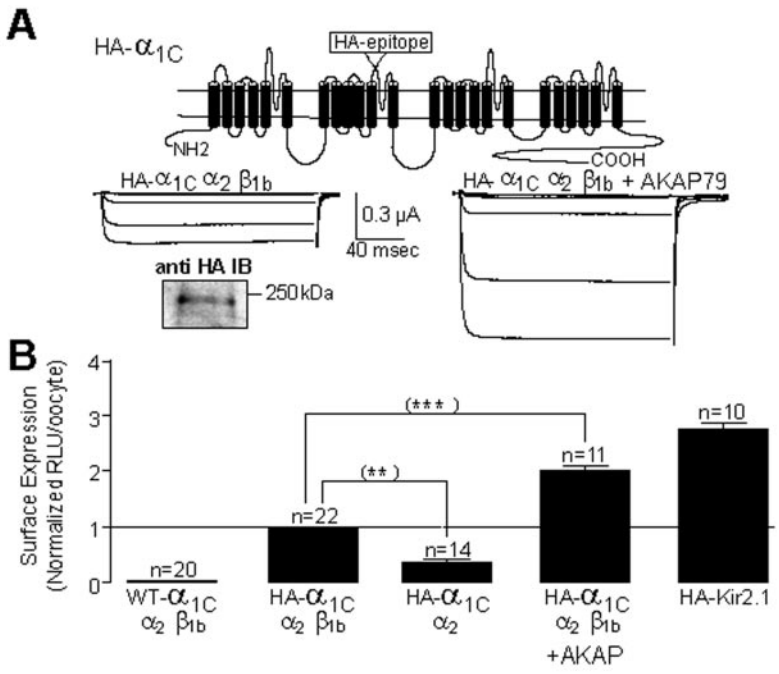

FIG. 3. **AKAP79 stimulates α_{1C} cell surface expression.** *A*, topological representation of HA-α_{1C} showing the site of insertion of the HA epitope and representative current traces in response to 200-millesecond long depolarizations from −80 mV to five successive steps to −40, −30, −20, −10, and 0 mV for HA-α_{1C} α_2-δ β_{1b} ± AKAP79. Note that AKAP79 induces an increase in whole cell currents similar to that seen with the WT channel. The Western blot (*inset*) illustrates recognition of the HA-α_{1C} protein by the anti-HA antibody. *B*, quantification of expression levels of tagged proteins on the surface of non-permeabilized cells was assessed by labeling with anti-HA primary and HRP-conjugated secondary antibodies. Single oocyte chemiluminescence was detected with a luminometer and reported as normalized relative light units (*RLU*) in the histogram. Note that co-expression of AKAP79 promotes an increase in surface expression of the HA-α_{1C} channel complex that is consistent with the observed stimulation of current density. All *error bars* shown denote S.E. *Asterisks* show statistical differences using Student's *t* tests.

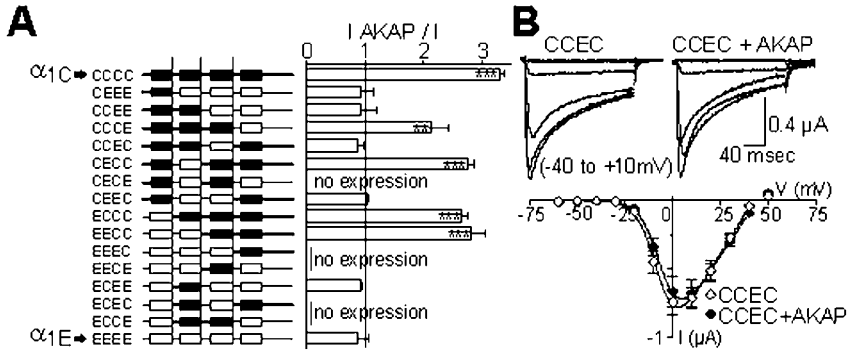

FIG. 4. **Channel structural determinants of AKAP79-sensitive trafficking.** *A*, the *left panel* shows the various chimeras combining the four transmembrane domains of α_{1C} (*filled rectangles*) and α_{1E} (*hollow rectangles*). The *right panel* shows the magnitude of AKAP effects obtained for these various channels. Chimeras that do not form functional channels are indicated and included for completeness. Note that AKAP stimulation is abolished only in the absence of domain III of α_{1C}. Data from 7 to 11 experiments per chimera are included in the figure. Statistical difference with data obtained for α_{1E} is indicated by *asterisks*. *B*, representative current traces and I/V curves for CCEC + α_2-δ + β_{1b} ± AKAP79 showing that chimera does not retain the AKAP trafficking effect (n = 9).

tained by replacement of domains I, II, or IV of α_{1C} with those of α_{1E} (ECCC, CECC, EECC, and CCCE). By contrast, substitution of domain III of α_{1C} abolished the AKAP79 effects (Fig. 4, *A* and *B*), implicating domain III and the associated II-III linker as a key determinant. Because cytoplasmic regions are the prime candidates for mediating interactions with intracellular proteins, we further studied the role of the II-III linker. We first examined whether overexpression of the α_{1C} II-III linker or subregions of this loop could act to inhibit the AKAP79 effect. These loops (as well as the corresponding re-

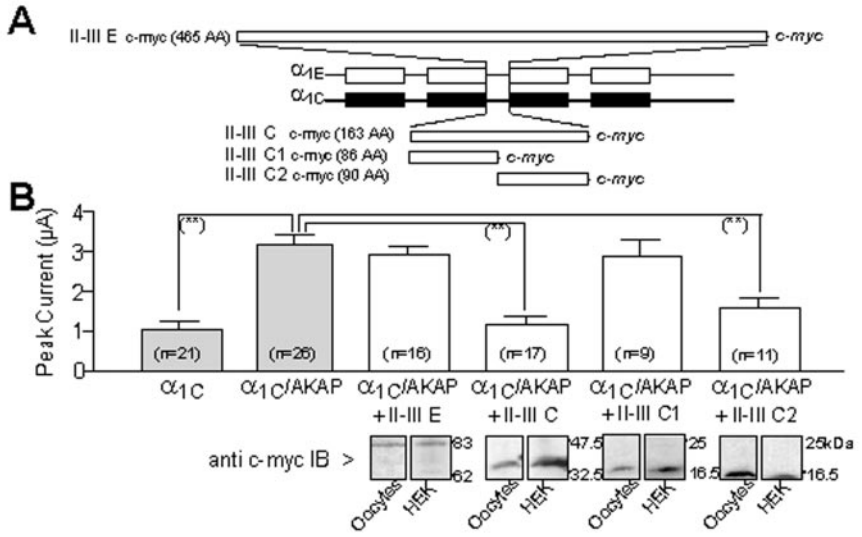

FIG. 5. **Overexpression of the α_{1C} II-III loop prevents AKAP79-mediated trafficking.** *A*, schematic representation of the II-III loop expression constructs that were fused to a c-*myc* epitope to verify expression. *B*, histograms illustrating the effect of coexpression of the various II-III loop proteins on the amplitude of α_{1C} + α_2-δ +β_{1b} currents in the presence of AKAP79. Note that II-III C and II-III C2 act as dominant negatives of the AKAP effect. *Inset*, Western blots illustrating the correct expression of the linker constructs. The Western blots were generated from oocytes subsequent to electrophysiological recordings. Note that the various linker proteins have the same size when expressed in HEK cells.

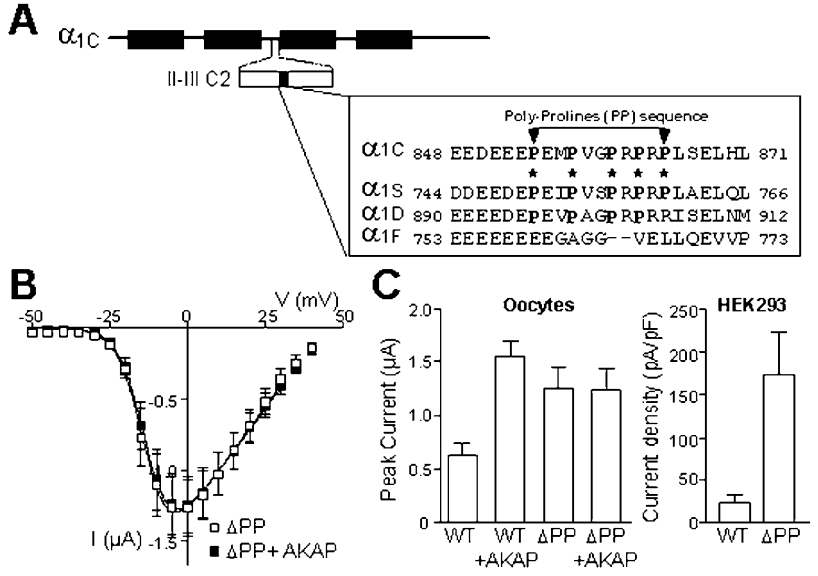

FIG. 6. *A*, primary sequence alignment of a proline-rich segment (*PP* region) within the II-III C2 segment of α_{1C} with corresponding regions of all Ca_V1 subunits, α_{1S}, α_{1D}, and α_{1F}. The *asterisks* show the proline residues conserved among α_{1C}, α_{1S}, and α_{1D}. This 11-amino acid cluster was deleted in $\alpha_{1C\ \Delta PP}$ mutant (Δ*PP*). *B*, I/V relationships for ΔPP + α_2-δ + β_{1b} ± AKAP79. Note that ΔPP is insensitive to the presence of AKAP79. *C*, summary of current amplitudes of wild-type α_{1C} (*WT*) or ΔPP channels (coexpressed with α_2-δ and β_{1b}) in the absence and presence of AKAP79 in oocytes (*left panel*, n = 16–24). Current density plot of WT and ΔPP channels (with α_2-δ and β_{1b}) in HEK cells (*right panel*, n = 7). Note that deletion of the proline-rich region increases current density toward levels obtained with wild-type α_{1C} with AKAP79.

gion of α_{1E} as a negative control) were fused to a c-Myc epitope in an expression vector (Fig. 5*A*), and their correct expression was verified by Western blot from oocytes used for electrophysiological recording. Protein sizes were confirmed by metabolic labeling (not shown) as well as by blotting the same proteins transiently expressed in HEK 293 cells (Fig. 5*B*). Using a 3:1 ratio of channel subunits AKAP79 to II-III loop, the expression of the α_{1E} II-III linker did not alter the magnitude of the AKAP79 effect. In contrast, the effect of AKAP79 was reduced to control levels in the presence of the α_{1C} II-III linker (Fig. 5*B*, *II-III C*). This effect appeared to be selectively due to the carboxyl half (*II-III C2*) of the domain II-III linker, suggesting that the presence of a possible interacting domain on II-III C and II-III C2 is able to quench the AKAP79 effect.

A Proline-rich Motif Restrains α_{1C} Surface Expression in the Absence of AKAP79—Upon examination of the amino acid sequence of the carboxyl half of the α_{1C} II-III linker, we noted a conspicuous polyproline motif (Fig. 6*A*, designated *PP* region) that is conserved in three of the four L-type calcium channel α_1 subunits identified to date. Because proline motifs are frequently implicated in protein-protein interactions, we deleted this 11-amino acid cluster containing the 5 prolines (to generate $\alpha_{1C\text{-}\Delta PP}$) and examined the ability of AKAP79 to enhance currents carried by the mutant channel. The deletion did not affect channel properties *per se*; however, it completely negated the AKAP79 effect (Fig. 6*B*). Interestingly, the deletion resulted in current densities that were similar to those seen with the WT channels coexpressed with AKAP79 (Fig. 6*C*). This effect was not confined to the *Xenopus* oocyte expression system, because an even larger increase (~8-fold) in current density was obtained when the channels were expressed in HEK cells (Fig. 6*C*). Overall, our data indicate that the PP region is antagonistic to channel surface expression and that AKAP79 may serve to counteract the role of the PP motif.

DISCUSSION

Ion channels do not operate as free floating entities in the plasma membrane but rather associate with intracellular molecules that are important for their trafficking to the membrane, their sorting toward subcellular sites, and their association with specific molecules to form specialized signal transduction complexes. A number of interacting partners have been recognized for various Ca^{2+} channel subunits (1). Membrane-bound AKAP proteins are part of L-type Ca^{2+} channel signaling networks (5, 8, 9, 11). The data presented here indicate that in addition to its known role on kinase and phosphatase regula-

tion, the postsynaptic scaffolding AKAP79 largely promotes surface expression of L-type Ca^{2+} channels.

It is now well established that the surface expression of plasma membrane proteins can be regulated by a number of specific sequences (28). These include quality control and forward trafficking signals that regulate supply to the membrane as well as internalization motifs that control protein retrieval from the surface by endocytosis. In our experiments we characterized an 11-amino acid cluster enriched in proline residues that mediates the AKAP79-induced surface expression. Although several ion channels contain well established endocytotic motifs, none of these such as the di-lysine or the tyrosine-based (YxxΦ) signals (29) are found in the α_{1C} cytoplasmic region identified as critical for the AKAP79-mediated effects. Increased surface expression resulting from an interaction of different constitutive subunits of a channel complex such as the one we describe here are more often linked to quality control mechanisms involving the shielding of endoplasmic reticulum retention/retrieval signals in the fully assembled channels (20, 30). Such a role has been described for the calcium channel β-subunit, which occludes a retention signal within the α_1 subunit domain I-II linker (26). Similarly, AKAP79 may act on the PP region of Ca_V1 channels by a similar mechanism, although this will be addressed in the future. Nonetheless, these data together with those of earlier studies (26, 31) suggest that individual calcium channels may contain a variety of surface expression determinants that differ among the three Ca_V subfamilies, providing a specific regulation of their cellular dynamic. We show here that only three Ca_V1 pore-forming subunits contain the PP region in their II-III loop. Similarly, the β-subunit occlusion of the I-II loop retention signal is likely restricted to Ca_V1 and Ca_V2 channels because members of the Ca_V3 family have divergent I-II linkers and are not regulated by β-subunits. AKAP79 has been shown to interact with a number of proteins, suggesting the possibility that it might physically bind to the PP region. However, we could not detect *in vitro* binding between AKAP79 and α_{1C} II-III-linker fusion proteins (not shown), indicating that AKAP79 and α_{1C} interact only weakly and perhaps only transiently, if at all. Alternatively, it is possible that AKAP79 might interact with the L-type calcium channel via one or more adaptor proteins, as reported for the AKAP79/AMPA receptor interaction (32). Nonetheless, future biochemical and molecular studies will be required to unravel all the details of these events to fully interpret the cell biological mechanism by which α_{1C} surface expression is enhanced.

From a physiological point of view, there is growing evidence that signaling pathways are structurally, spatially, and temporally tightly regulated. Biochemical data obtained from intact neurons have shown that the murine homologue of AKAP79 (AKAP150) interacts with α_{1C} and the β2-adrenergic receptor in dendritic spines, possibly implicating AKAPs in receptor signaling to L-type calcium channels via PKA (16, 33). Within the context of this colocalization, however, our data suggest a novel role of AKAP79 in calcium channel modulation that occurs independently of PKA signaling. At the same time, AKAP79 may promote the association of molecular complexes comprising L-type Ca^{2+} channels and lead to their preferential trafficking/targeting to postsynaptic dendritic spines, as well as enhance calcium current densities. In view of the physiological role of L-type calcium channels in the activation of calcium-dependent enzymes and, perhaps more importantly, the triggering of calcium-dependent gene transcription (34), a dynamic regulation of L-type calcium channel levels via AKAP proteins may provide an important feedback mechanism for regulating these processes via controlling L-type channel surface expression. Furthermore, like L-type channels, AKAP79/150 proteins have been shown to stimulate cAMP-response element-binding protein-dependent gene transcription (35, 36), suggesting the intriguing possibility that AKAPs could be part of the signaling cascade between L-type calcium channels and the nucleus that is preferentially activated at postsynaptic sites (37).

Acknowledgments—We thank Terry P. Snutch, Arnaud Monteil, and Edward Perez Reyes for providing wild-type calcium channel subunit cDNAs, Manfred Grabner and Kurt G. Beam for the green fluorescent protein-tagged α_1 subunits, and Caroline Dart for the HA-Kir2.1 construct. We thank François Rassendren for help and suggestions, Blanche Schwappach for sharing protocols, Adeline Burgiere and Caroline Perron for technical help, and Philippe Lory for careful reading of the manuscript. The North Atlantic Treaty Organization provided travel support.

REFERENCES

1. Catterall, W. A. (2000) *Annu. Rev. Cell Dev. Biol.* **16,** 521–555
2. Ertel, E. A., Campbell, K. P., Harpold, M. M., Hofmann, F., Mori, Y., Perez-Reyes, E., Schwartz, A., Snutch, T. P., Tanabe, T., Birnbaumer, L., Tsien, R. W., and Catterall, W. A. (2000) *Neuron* **25,** 533–535
3. Johnson, B. D., Scheuer, T., and Catterall, W. A. (1994) *Proc. Natl. Acad. Sci. U. S. A.* **91,** 11492–11496
4. Zhong, J., Hume, J. R., and Keef, K. D. (1999) *Am. J. Physiol.* **277** (4 Pt 1), C840–844
5. Gao, T., Yatani, A., Dell'Acqua, M. L., Sako, H., Green, S. A., Dascal, N., Scott, J. D., and Hosey, M. M. (1997) *Neuron* **19,** 185–196
6. Sculptoreanu, A., Scheuer, T., and Catterall, W. A. (1993) *Nature* **364,** 240–243
7. Fink, M. A., Zakhary, D. R., Mackey, J. A., Desnoyer, R. W., Apperson-Hansen, C., Damron, D. S., and Bond, M. (2001) *Circ. Res.* **88,** 291–297
8. Gray, P. C., Johnson, B. D., Westenbroek, R. E., Hays, L. G., Yates, J. R., III, Scheuer, T., Catterall, W. A., and Murphy, B. J. (1998) *Neuron* **20,** 1017–1026
9. Fraser, I. D., Tavalin, S. J., Lester, L. B., Langeberg, L. K., Westphal, A. M., Dean, R. A., Marrion, N. V., and Scott, J. D. (1998) *EMBO J.* **17,** 2261–2272
10. Charnet, P., Lory, P., Bourinet, E., Collin, T., and Nargeot, J. (1995) *Biochimie (Paris)* **77,** 957–962
11. Hulme, J. T., Ahn, M., Hauschka, S. D., Scheuer, T., and Catterall, W. A. (2001) *J. Biol. Chem.* **30,** 30
12. Hell, J. W., Westenbroek, R. E., Warner, C., Ahlijanian, M. K., Prystay, W., Gilbert, M. M., Snutch, T. P., and Catterall, W. A. (1993) *J. Cell Biol.* **123,** 949–962
13. Carr, D. W., Stofko-Hahn, R. E., Fraser, I. D., Cone, R. D., and Scott, J. D. (1992) *J. Biol. Chem.* **267,** 16816–16823
14. Glantz, S. B., Amat, J. A., and Rubin, C. S. (1992) *Mol. Biol. Cell* **3,** 1215–1228
15. Dell'Acqua, M. L., Faux, M. C., Thorburn, J., Thorburn, A., and Scott, J. D. (1998) *EMBO J.* **17,** 2246–2260
16. Davare, M. A., Avdonin, V., Hall, D. D., Peden, E. M., Burette, A., Weinberg, R. J., Horne, M. C., Hoshi, T., and Hell, J. W. (2001) *Science* **293,** 98–101
17. Spaetgens, R. L., and Zamponi, G. W. (1999) *J. Biol. Chem.* **274,** 22428–22436
18. Stotz, S. C., and Zamponi, G. W. (2001) *J. Biol. Chem.* **276,** 33001–33010
19. Altier, C., Spaetgens, R. L., Nargeot, J., Bourinet, E., and Zamponi, G. W. (2001) *Neuropharmacology* **40,** 1050–1057
20. Zerangue, N., Schwappach, B., Jan, Y. N., and Jan, L. Y. (1999) *Neuron* **22,** 537–548
21. Sharp, A. H., Black, J. L., Dubel, S. J., Sundarraj, S., Shen, J., Yunker, A. M., Copeland, T. D., and McEnery, M. W. (2001) *Neuroscience* **105,** 599–617
22. Colledge, M., and Scott, J. D. (1999) *Trends Cell Biol.* **9,** 216–221
23. Carr, D. W., Stofko-Hahn, R. E., Fraser, I. D., Bishop, S. M., Acott, T. S., Brennan, R. G., and Scott, J. D. (1991) *J. Biol. Chem.* **266,** 14188–14192
24. Dodge, K., and Scott, J. D. (2000) *FEBS Lett.* **476** (1–2), 58–61
25. Schwake, M., Pusch, M., Kharkovets, T., and Jentsch, T. J. (2000) *J. Biol. Chem.* **275,** 13343–13348
26. Bichet, D., Cornet, V., Geib, S., Carlier, E., Volsen, S., Hoshi, T., Mori, Y., and De Waard, M. (2000) *Neuron* **25,** 177–190
27. Canti, C., Davies, A., Berrow, N. S., Butcher, A. J., Page, K. M., and Dolphin, A. C. (2001) *Biophys. J.* **81,** 1439–1451
28. Ma, D., Zerangue, N., Raab-Graham, K., Fried, S. R., Jan, Y. N., and Jan, L. Y. (2002) *Neuron* **33,** 715–729
29. Madrid, R., Le Maout, S., Barrault, M. B., Janvier, K., Benichou, S., and Merot, J. (2001) *EMBO J.* **20,** 7008–7021
30. Zerangue, N., Malan, M. J., Fried, S. R., Dazin, P. F., Jan, Y. N., Jan, L. Y., and Schwappach, B. (2001) *Proc. Natl. Acad. Sci. U. S. A.* **98,** 2431–2436
31. Gao, T., Bunemann, M., Gerhardstein, B. L., Ma, H., and Hosey, M. M. (2000) *J. Biol. Chem.* **275,** 25436–25444
32. Colledge, M., Dean, R. A., Scott, G. K., Langeberg, L. K., Huganir, R. L., and Scott, J. D. (2000) *Neuron* **27,** 107–119
33. Hall, D. D., Davare, M. A., Avdonin, V., Peden, E. M., Burette, A., Weinberg, R. J., Horne, M. C., Hoshi, T., and Hell, J. W. (2001) A. 271.9, Society for Neuroscience meeting, San Diego, CA
34. Dolmetsch, R. E., Pajvani, U., Fife, K., Spotts, J. M., and Greenberg, M. E. (2001) *Science* **294,** 333–339
35. Feliciello, A., Li, Y., Avvedimento, E. V., Gottesman, M. E., and Rubin, C. S. (1997) *Curr. Biol.* **7,** 1011–1014
36. Cassano, S., Di Lieto, A., Cerillo, R., and Avvedimento, E. V. (1999) *J. Biol. Chem.* **274,** 32574–32579
37. Deisseroth, K., Bito, H., and Tsien, R. W. (1996) *Neuron* **16,** 89–101